

Style-Adaptive Detection Transformer for Single-Source Domain Generalized Object Detection

Jianhong Han, *Student Member, IEEE*, Yupei Wang*, *Member, IEEE*, Liang Chen, *Member, IEEE*

Abstract—Single-source Domain Generalization (SDG) in object detection aims to develop a detector using only data from source domain that can exhibit strong generalization capability when applied to other unseen target domains. Existing methods are built upon CNN-based detectors and primarily improve their robustness by employing carefully designed data augmentation strategies integrated with feature alignment techniques. However, the data augmentation methods have inherent drawbacks that are only effective when the augmented sample distribution approximates or covers the unseen scenarios, thus failing to enhance the detector’s generalization capability across all unseen scenarios. Furthermore, while the recent DETection TRansformer (DETR) has demonstrated superior generalization capability in domain adaptation tasks due to its efficient global information extraction, its potential in SDG tasks still remains unexplored. To this end, we introduce a strong DETR-based detector named the Style-Adaptive DETection TRansformer (SA-DETR) for SDG in object detection. Specifically, we present a domain style adapter to project the style representation of the unseen target domain into the training domain, enabling dynamic style adaptation across various unseen scenarios. Then, the object-aware contrastive learning module is proposed to force the detector to extract domain-invariant features of objects through contrastive learning. By employing carefully designed object-aware gating masks to constrain the scope of feature aggregation in both spatial position and semantic category, this module effectively achieves cross-domain contrast of instance-level features, thereby further enhancing the detector’s generalization capability. Extensive experimental results demonstrate the superior performance and generalization capability of our proposed SA-DETR across five different weather scenarios. Code is released at <https://github.com/h751410234/SA-DETR>.

Index Terms—Single-source domain generalization (SDG), object detection, detection transformer.

I. INTRODUCTION

THE task of Single-source Domain Generalization (SDG) is designed to mitigate domain gaps that arise from distribution differences between the training data (source domain) and real-world application data (target domain). Unlike traditional unsupervised domain adaptation tasks [1]–[3], which

allow the use of images from the target domain, SDG enhances the robustness of networks to various unseen target scenarios by using only data from a single-source domain. Although this task is more difficult, it has been receiving increasing attention because it better aligns with practical deployment requirements, such as autonomous driving.

Recently, many methods [4]–[6] for SDG in object detection have been proposed, employing carefully designed generalization strategies to enhance the robustness of detectors, but they overlook two significant issues. Firstly, to overcome the limited sample space of single-source domain data, existing methods typically employ innovative data augmentation strategies (at the image or feature level) to obtain more diverse samples for training, thereby enhancing the generalization capability of detectors for unseen scenarios. However, these methods have inherent drawbacks that are only effective when the augmented sample distribution approximates or covers the unseen scenarios. Due to the unpredictable deployment environments, which are likely to have significant differences from the augmented samples, the improvement in detector performance is minimal in such cases.

Secondly, researchers have primarily explored and demonstrated effectiveness within the Faster R-CNN [7], while transformer-based detectors have been less studied. Recent works [8]–[10] increasingly shows that detectors based on the DETection TRansformer (DETR) [11] exhibit superior performance in handling domain gaps compared to those based on Convolutional Neural Networks (CNNs). Unlike purely convolutional designs, DETR innovatively integrates a CNN backbone with transformer architecture (i.e., encoder and decoder), leveraging the attention mechanism to refine features for more detailed representations [12]. Additionally, the transformer architecture has been proven to be highly effective in capturing global structural information [13], [14], potentially offering better generalization capability for unseen scenarios. Therefore, it is highly meaningful to explore the effectiveness of DETR-based detectors in addressing the SDG task.

In this paper, we introduce a strong DETR-based detector named the Style-Adaptive DETection TRansformer (SA-DETR) for SDG in object detection. To better adapt to unseen scenarios, we designed a domain style adapter that projects the style representation of the unseen target domain into the training domain. Unlike methods that expand data space, our adapter establishes a new avenue that utilizes known data to represent unseen ones, thereby enabling dynamic style

This work was supported by the MYHT Program under Grant D040404, National Key Research and Development Program of China under Grant 2023YFC3605904, National Key Laboratory for Space-Born Intelligent Information Processing under Grant TJ-01-22-01. (*Corresponding author: Yupei Wang.*)

J. Han, Y. Wang and L. Chen are with the School of Information and Electronics, Beijing Institute of Technology, Beijing 100081, China, also with the Beijing Institute of Technology Chongqing Innovation Center, Chongqing 401135, China, and also with the National Key Laboratory for Space-Born Intelligent Information Processing, Beijing 100081, China. E-mail: hanjianhong1996@163.com, wangyupei2019@outlook.com, chenl@bit.edu.cn.

Manuscript submitted to IEEE Transactions on Multimedia.

adaptation across various unseen scenarios. Specifically, we use a memory module to store the statistical data (mean and variance) of feature maps extracted from the backbone during each training iteration. These data are naturally considered to be prototypical features of image styles, similar to those used in style transfer techniques [15]–[17]. As the stored prototypes accumulate, the memory module can develop dataset-level style representations, which we use as the style basis to rectify the style of the unseen images. During inference, we first calculate the Wasserstein distance [18] between the statistical data of the input image and the stored prototypes to estimate the style distribution discrepancy. Then, this distance is used as weighting factors, integrated within the AdaIN function [19] to facilitate an accurate projection.

To further enhance the generalization capability, we have introduced an object-aware contrastive learning module that forces the detector to extract domain-invariant features of objects through contrastive learning. Differing from the proposed adapter that addresses the SDG challenge at the image level, this module employs carefully designed object-aware gating masks to constrain the scope of feature aggregation in both spatial position and semantic category, thereby effectively achieving cross-domain contrast (i.e., between the source domain and the augmented domain) of instance-level features. Specifically, we insert multiple class queries into the transformer encoder, with each query responsible for capturing features of a specific category. Utilizing object-aware gating masks created from annotations, these queries adaptively aggregate specific positional and categorical features from the feature tokens by leveraging a cross-attention mechanism. Then, we introduce a contrastive learning to minimize the differences among these aggregated queries, which can be considered instance-level prototypes for each category. By attracting prototypes of the same category and repelling those of different categories across domains, the detector is forced to extract domain-invariant object features, thereby enhancing its generalization capability.

The main contributions of this paper are as follows:

- We show that DETR-based detectors exhibit better generalization in unseen scenarios, and propose a style-adaptive detection transformer. To the best of our knowledge, this is the first work that explores the benefit of a DETR-based detector for the single-source domain generalization task.
- We present a novel domain style adapter which projects the style representation of the unseen target domain into the training domain, enabling dynamic style adaptation across various unseen scenarios. The adapter establishes a new avenue for addressing the challenge of single-source domain generalization in object detection.
- To further enhance the generalization capability, an object-aware contrastive learning module is introduced. This module employs carefully designed object-aware gating masks to constrain the scope of feature aggregation in both spatial position and semantic category, thus forcing the detector to extract domain-invariant features of objects.

Extensive results demonstrate the superior performance and generalization capability of SA-DETR compared to state-of-the-art methods across five different weather conditions. Our results consistently achieved the best outcomes in all scenarios and showed a remarkable 12.2% improvement in mAP on the "Dusk-Rainy" scene.

II. RELATED WORK

A. *The Preliminaries of Detection Transformer*

Following the success of the Transformer architecture [20], Carion et al. [11] integrated this architecture into an object detection method named DEtection TRansformer (DETR). Unlike traditional convolutional designs, DETR uses encoders to further refine features extracted from the backbone network and employs multiple object queries to obtain detection results in the decoder. This approach significantly simplifies the detection pipeline by eliminating the need for manually designed anchors [7] and Non-Maximum Suppression (NMS) [21]. Recently, many researchers [22]–[24] have investigated the potential of DETR-based detectors in addressing domain adaptation challenges, given that the transformer architecture excels at capturing global structural information. However, for domain generalization in object detection, existing methods still build on fully convolutional two-stage architectures like Faster R-CNN [7]. In this paper, we showcase the superior generalization capability of DETR-based detectors in unseen scenarios and introduce a style-adaptive detection transformer. To the best of our knowledge, this is the first study to explore the benefit of a DETR-based detector for the single-source domain generalization task.

B. *Domain Adaptation and Generalization*

The domain gap is a common issue encountered during network deployment, caused by differences in the distribution between collected data (source domain) and real-world application data (target domain). Current deep learning methods, limited by data-driven supervised learning architectures, often experience significant performance degradation when facing such domain gaps. To address this, domain adaptation techniques [25]–[27] have been proposed that leverage unlabeled (unsupervised) or minimal (few-shot learning) target domain samples to mitigate the domain gap. Unlike domain adaptation, which assumes access to target domain images during training, the domain generalization task aims to enhance a model's generalization capability to adapt to completely unseen scenarios, making it a more challenging but more practically relevant problem for real-world deployment. In this paper, we address the issue of domain generalization in object detection and focus on using data from a single-source domain.

C. *Single-source Domain Generalization for Object Detection*

Single-source Domain Generalization (SDG), a specific case of domain generalization task, aims to enhance network performance on unseen scenarios using only data from one source domain. At present, most research on SDG has concentrated on image classification [28]–[30] and segmentation [31]–[33],

with limited work in the field of object detection, which warrants further exploration. Existing approaches primarily enhance the detector’s generalization capability by implementing data augmentation strategies and feature alignment techniques.

For data augmentation strategies, the methods are similar to those used in image classification. IBN-Net [34] and ISW [35] utilize instance normalization and whitening on extracted features to mitigate the impact of specific domain styles. Then, CLIP-Gap [5] employs the pre-trained vision-language model CLIP [36], using carefully designed text prompts to improve the semantic style features extracted from the backbone. Additionally, MAD [37] transfers input images to the frequency domain and randomizes the distribution of extremely high and low-frequency components to increase the diversity of source domain data. Building on this, UFR [6] incorporates SAM [38] to isolate targets within images for further augmentation. Unlike the aforementioned methods, our proposed domain style adapter projects the style representations of the unseen target domain into the training domain, enabling dynamic style adaptation across various unseen scenarios.

Feature alignment techniques are usually applied in SDG for object detection to further alleviate the influence of the domain gap. These techniques align cross-domain features by utilizing data from both the source and augmented domains, thereby facilitating the extraction of domain-invariant features in the detector. SDGOD [4] introduces a cyclic-disentangled self-distillation framework that achieves domain-invariant feature extraction without annotated labels. MAD [37] proposes a multi-view adversarial discriminator to achieve more precise alignment of cross-domain features. To complement the image-level feature alignment methods discussed above, UFR [6] has developed a causal prototype learning module that refines features extracted from Regions Of Interest (ROI) to further mitigate the influence of confounding factors in object attributes. Since the proposed adapter effectively addresses the image-level domain gap, we introduce an object-aware contrastive learning module to further encourage the DETR-based detector to extract domain-invariant instance-level features. This module employs carefully designed object-aware gating masks to constrain contrastive learning on instance-level features, thereby achieving accurate cross-domain feature alignment for objects.

III. METHOD

SA-DETR is a strong DETR-based detector for single-source domain generalization in object detection. In this section, we first provide a framework overview, which includes the DETR revisit, the data augmentation method and the framework of our detector. Then, we detail the proposed domain style adapter and the object-aware contrastive learning module in subsequent sections. Finally, the loss functions used in our method are described in the overall training objective section.

A. Framework Overview

DETR revisit. In our approach, we utilize DINO [39] as the base detector, an advanced DETR-based end-to-end object

detector. Specifically, DINO incorporates a CNN backbone for feature extraction and employs an encoder-decoder transformer structure along with a detection head for the final detection predictions. When processing an image, the backbone initially extracts multi-scale feature maps similar to those used in CNN-based detectors. These feature maps are then reshaped into feature tokens that feed into the encoder-decoder module. The encoder further refines the input features by using self-attention. The decoder uses inserted object queries to probe local regions and aggregate instance features from the refined features through cross-attention, generating output embeddings. Finally, these output embeddings are used to compute prediction results through the detection head.

Data augmentation. The objective of single-source domain generalization is to train the network with data from a single domain and to generalize its performance to a variety of unseen scenarios. In this task, data augmentation methods are essential to break the limitations of sample diversity. Inspired by previous work [37], we employ spurious correlation generator to augment the source dataset at the image level, ultimately yielding an augmented dataset of equivalent size. Therefore, the input to our method includes both the source and augmented data. Building upon this foundation, we propose the domain style adapter to leverage known styles for representing unseen ones, thereby overcoming the limitations of augmentation methods in improving performance.

Framework. As shown in Fig. 1 (a), Our SA-DETR adopts DINO as the base detector and integrates our designed methods, including a Domain Style Adapter (DSA) and an Object-aware Contrastive Learning (OCL) module. Specifically, during training, the network inputs consist of pairs of images, each pair containing an equal number of images from both the source and augmented domains. For a batch of image pairs, the detector first uses a ResNet backbone [40] to extract multi-scale feature maps, and feeds the maps from each layer into our proposed adapter. The adapter stores the statistical data of the input features using a memory module and forms them into two domain-style bases. Then, the extracted feature maps are further refined in the encoder. Meanwhile, we insert an OCL module into the encoder, which utilizes contrastive learning to force the extraction of domain-invariant features of objects, thereby enhancing the detector’s generalization capability. Ultimately, the refined features are input into the subsequent decoder and detection head to obtain detection results, in line with DINO. During inference, the adapter rectifies the channel statistical characteristics of the backbone’s extracted feature maps using the stored style base, effectively projecting the style representations of the unseen domain into the training domain. Notably, our OCL module is employed only during training as a plugin. More details on the DSA and the OCL module will be presented in Subsections III-B and III-C, respectively.

B. Domain Style Adapter

Previous works have adopted data augmentation to increase dataset diversity and then trained on the mixed data to generalize the network. However, these methods are effective

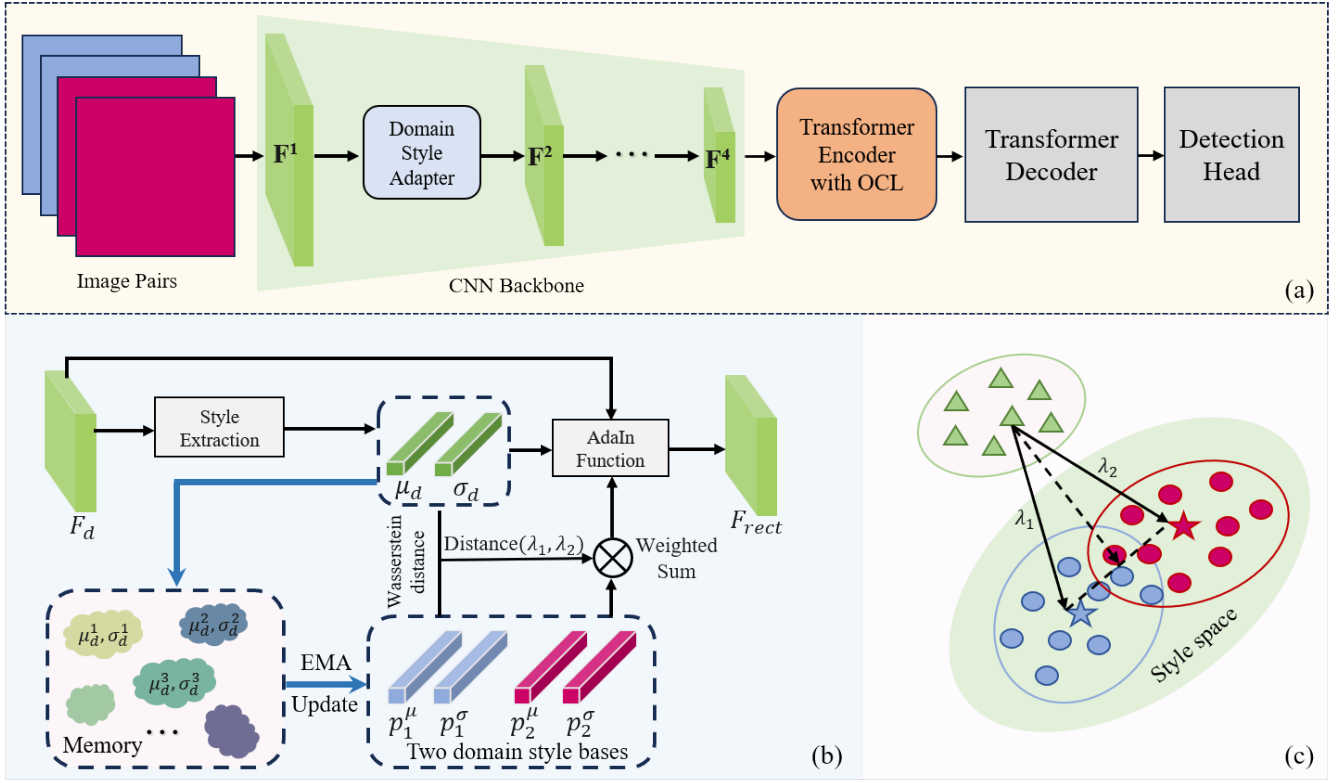


Fig. 1. Details of (a) the overview of the proposed SA-DETR framework, which adopts DINO as the base detector and incorporates a Domain Style Adapter (DSA) and an Object-Aware Contrastive Learning (OCL) module, and (b) the workflow of the DSA. Meanwhile, the memory module is only used during training to store statistical data of input features and to form a style base, as indicated by the blue arrows. (c) illustrating the projection process during inference, where red and blue respectively represent the source and augmented domains, and green represents the unseen target domain. The adapter rectifies the channel statistical characteristics of the backbone’s extracted feature maps using the stored style base, effectively projecting the style representations of the unseen target domain into the training domain.

only when the augmented sample distributions closely match the unseen scenarios, as detailed in the experimental section IV-C. Inspired by style transfer techniques [16], [31], [41], we propose a domain style adapter that projects the style representation of the target domain into the training domain for dynamic style adaptation across various unseen scenarios.

Given the feature map of a specific layer $F_d \in \mathbb{R}^{(B \times C \times H \times W)}$ (where d denotes the domain of the input image, either the source domain or the augmented domain), we first compute its statistical data, i.e., the mean μ_d and variance σ_d along the channel dimension, as follows:

$$\mu_d(F_d) = \frac{1}{HW} \sum_{h=1}^H \sum_{w=1}^W F_d, \quad (1)$$

$$\sigma_d(F_d) = \sqrt{\frac{1}{HW} \sum_{h=1}^H \sum_{w=1}^W (F_d - \mu_d(F_d))^2 + \epsilon}, \quad (2)$$

where μ_d and $\sigma_d \in \mathbb{R}^{(B \times C)}$, ϵ is set to 1×10^{-6} to avoid numerical computation resulting in zero. Since the network’s input consists of image pairs, we calculate the mean and variance for both the source and the augmented domain images, respectively.

Then, we store the means and variances for each domain using a memory module during each training iteration and

utilize the Exponential Moving Average (EMA) [42] method to generate domain-specific style bases online, as detailed below:

$$p_d^\mu = \alpha p_d^\mu + (1 - \alpha) \mu_d, \quad (3)$$

$$p_d^\sigma = \alpha p_d^\sigma + (1 - \alpha) \sigma_d, \quad (4)$$

where α represents the momentum factor, which is normally close to 1. Both p_d^μ and p_d^σ are initialized to zero. As the stored statistical data accumulate, the memory module can develop dataset-level style represents.

After the calculations described above, we obtain two style bases corresponding to the source and augmented domains. Subsequently, we use these bases to rectify the style of the input image, projecting the style representation of the target domain into the training domain. Specifically, we use the Wasserstein distance [18] to measure the distribution differences in the statistical data between the current image and the two stored bases to obtain the correlation coefficient, as follows:

$$\lambda_d = \|\mu_d - p_d^\mu\|_2^2 + (\sigma_d^2 + p_d^{\sigma^2} - 2\sigma_d p_d^\sigma), \quad (5)$$

where λ_d represents the distribution distance between the current image and the stored bases for each domain d . Given that our training images are confined to the source and augmented domains, we define the set λ as $\{\lambda_1, \lambda_2\}$. The set λ is processed by a softmax operation to ensure the values sum

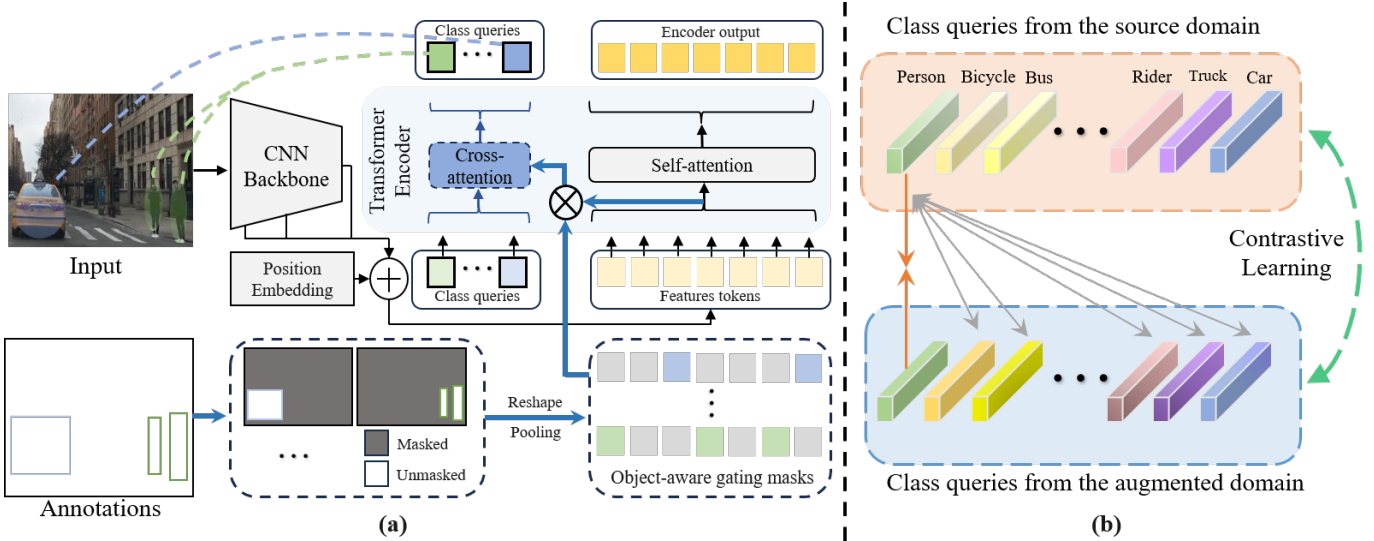


Fig. 2. Our proposed object-aware contrastive learning (OCL) module. Details of (a) the inserted class queries adaptively capture features of objects by utilizing the generated object-aware gating masks, and (b) cross-domain instance-level feature alignment is achieved by leveraging contrastive learning.

to 1, which are then used as weighting factors in the AdaIN function [19] to guide feature rectification, as detailed below:

$$\mu' = \text{softmax}(\lambda) \cdot p^\mu, \sigma' = \text{softmax}(\lambda) \cdot p^\sigma, \quad (6)$$

$$F_{rect} = \frac{F - \mu}{\sigma} \sigma' + \mu', \quad (7)$$

where F represents the original feature map of the input image, F_{rect} corresponds to its rectified feature map, “ \cdot ” denotes matrix multiplication. We rectify every layer of the extracted multi-scale feature maps during both the training and inference phases to ensure a consistent workflow in the detector.

C. Object-aware Contrastive Learning Module

Since DETR-based detectors lack region proposals, we leveraged the characteristics of the single-source domain generalization task, where both the source and augmented domains are labeled, to generate object-aware gating masks. By using these masks to filter out the aggregation of irrelevant features, we can accurately implement cross-domain contrast (i.e., between the source domain and the augmented domain) of instance-level features. The module structure is shown in Fig. 2.

Object-aware gating masks. We used the bounding boxes and their corresponding classes from the annotations to generate object-aware gating masks. Specifically, let $Y = \{(b_1, c^1), (b_2, c^2), \dots, (b_m, c^m)\}$ represent the annotations, where b_m and c^m denote the bounding box and category of the m -th object, respectively. We first aggregate all instances of the same category to obtain the coordinate set $B^c = \{b_1^c, b_2^c, \dots, b_i^c\}$, where each b includes two coordinates represented as $(x_{min}, y_{min}, x_{max}, y_{max})$. Then, we generate the gating masks based on the coordinate set B^c as follows:

$$g_{x,y}^c = \begin{cases} 1, & \text{if } x_{min} \leq x \leq x_{max} \text{ and } y_{min} \leq y \leq y_{max}; \\ 0, & \text{otherwise.} \end{cases} \quad (8)$$

We use $G^c = \{g_{x,y}^c\}_{H \times W}$ to denote the gating mask corresponding to category c , where $g_{x,y}^c = 1$ indicates that the current pixel position contains the object, and occlusion calculation of the attention mechanism is not required. Finally, we need to perform multi-scale downsampling and concatenation on the obtained gating masks to ensure alignment with the positions of the feature tokens input into the encoder.

Instance-level feature aggregation with class queries. We insert c class queries $Q = \{q_1, q_2, \dots, q_c\}$ into the encoder, with each query $q_i \in \mathbb{R}^d$ being a learnable vector designed to aggregate features of a specific category using a cross-attention mechanism. The scope of aggregation is controlled by the object-aware gating masks previously obtained, enabling aggregation solely for instance-level features. Specifically, we define the feature tokens as T , with corresponding position encodings P , and object-aware gating masks as $M = \{G^1, G^2, \dots, G^c\}$. In each transformer block of the encoder, all class queries Q are updated in parallel through cross-attention with the feature tokens, as follows:

$$Q^l = Q^{l-1} + \text{CrossAtten}(Q^{l-1}, T^{l-1} + P, T^{l-1}, M), \quad (9)$$

where $\text{CrossAtten}(\text{query}, \text{key}, \text{value}, \text{key_padding_mask})$ denotes the standard cross-attention layer, the superscript l represents the l -th block of the encoder. Ultimately, we obtain the class queries Q that aggregate instance-level features of each category.

Contrastive learning for feature alignment. Since the input images to our method include both the source and augmented domains, we can obtain class queries from two distinct domains. By attracting positive sample pairs (queries from the same category across both domains) and repelling negative samples, the detector is compelled to extract domain-invariant features from objects. Specifically, we define Q^S and $Q^A \in \mathbb{R}^{C \times d}$ as class query sets from the source and augmented domains, respectively. The contrastive learning loss

TABLE I
ABLATION STUDY OF SA-DETR

Model Component			mAP_{50}				
			Source domain		Unseen target domain		
Augmentation	DSA	OCL	Daytime-Clear	Daytime-Foggy	Dusk-Rainy	Night-Rainy	Night-Clear
			61.6	38.0	35.7	17.3	43.7
✓			62.6	41.1	36.0	17.6	44.8
	✓		62.0	38.6	42.8	21.1	41.9
✓	✓		63.8	41.7	44.2	22.2	44.7
✓	✓	✓	64.8	42.6	45.4	23.0	46.0

is constructed as follows:

$$L_{contra} = -\frac{1}{C} \sum_{i=1}^C \log \frac{\exp(q_i^S \cdot q_i^A)}{\sum_{j=1}^C \exp(q_j^S \cdot q_i^A)}, \quad (10)$$

where “.” is used to measure the similarity between queries from different domains, and C represents the total number of categories in the dataset. We calculate the loss in each block of the encoder.

D. Overall Training Objective

Since our OCL module employs contrastive learning to further enhance the generalization capability of the detector, the SA-DETR is trained using two types of loss functions: the supervised detection loss L_{det} , which is consistent with the DINO, and the contrastive learning loss L_{contra} as defined in Eq. (10). The training objective can be defined as follows:

$$L = L_{det} + \lambda_c L_{contra}, \quad (11)$$

where L_{det} and L_{contra} are used for both the source images and the augmented images, and λ_c denotes the balancing weights for the corresponding learning loss functions.

IV. EXPERIMENTS

This section details our experiments, including Datasets, Implementation Details and Evaluation Metrics, Ablation Studies, Comparisons with State-of-the-Art, and Visualization and Analysis. Detailed discussions of each aspect are provided in the following subsections.

A. Datasets

Following [4], [6], we employed a benchmark for single-source domain generalization in object detection to evaluate the SA-DETR. The dataset consists of scenes under five different weather conditions, meticulously selected from three public datasets: Berkeley Deep Drive 100K (BDD-100K) [43], Cityscapes [44], and Adverse-Weather [45]. Specifically, the experiment designated “Daytime-Clear” as the source domain, which includes 19,395 training images and 8,313 testing images. The other four conditions, used exclusively for testing as unseen scenarios, included “Daytime-Foggy” with 3,775 test images, “Dusk-Rainy” with 3,501 test images, “Night-Clear” with 26,158 test images, and “Night-Rainy” with 2,494 test images. All datasets encompassed seven categories: person, car, bike, rider, motor, bus, and truck.

B. Implementation Details and Evaluation Metric

Our approach is based on the DINO detector and is compared with existing methods. To ensure a fair comparison, we use ResNet-50 [40] as the backbone. In all experiments, our method employed a 1x training configuration, was trained in just 12 epochs, and achieved outstanding performance. For all scenarios, we set the weight factors λ_c in Eq. (11) to 0.1. Consistent with DINO’s settings, we trained our models using the Adam optimizer [46] with a base learning rate of 2×10^{-4} , which was reduced by a factor of 0.1 in the 11-th epoch. We conduct each experiment on an NVIDIA A6000 GPU with 48 GB of memory.

We use the mean Average Precision (mAP) to evaluate our method, as follows:

$$mAP = \frac{1}{c} \sum_{i=0}^c AP_i, \quad (12)$$

where $AP = \int_0^1 P(R) dR$ represents the area under the precision-recall curve and c denotes the number of categories. Consistent with the evaluation of other methods, we calculate the object detection evaluation metric at an IoU threshold of 50%.

C. Ablation Studies

In this section, we conducted ablation studies by selectively removing components to demonstrate their contributions, and the results are presented in Table I. First, we compared the performance before and after data augmentation to demonstrate that augmentation methods are suboptimal in enhancing the generalization of detection when significant scene differences are encountered. As shown in rows 1 and 2 of the table, “Augmentation” refers to the data augmentation method [37], which demonstrates limited effectiveness in enhancing performance in scenarios such as “Dusk-Rainy” and “Night-Rainy”. Subsequently, the results in row 3 show that our proposed Domain Style Adapter (DSA) achieved a satisfactory performance improvement in the aforementioned challenging scenarios, effectively complementing the augmentation method. Consequently, by integrating these two methods, the generalization of the detector is substantially enhanced across all unseen scenarios, as presented in row 4. To further enhance the generalization of the detector, we propose the Object-aware Contrastive Learning (OCL) module. Unlike the

proposed adapter that addresses the SDG challenge at the image level, this module improves the detector’s generalization by encouraging the extraction of domain-invariant instance-level features. As shown in row 5, the detector’s performance is further improved across various scenarios by incorporating the OCL module. Ultimately, our SA-DETR achieves significant improvements in all experimental scenarios compared to the vanilla DINO detector, demonstrating that the proposed components effectively enhance the detector’s generalization.

D. Comparisons with the State-of-the-Art

Following [4], [6], all methods are trained on the “Daytime-Clear” dataset and tested on five different weather scenarios. In each scenario, we compare our method with state-of-the-art SDG methods to demonstrate its effectiveness and generalization capability. Furthermore, we show the performance of the vanilla DINO to highlight the superior generalization of DETR-based detectors in some unseen scenarios.

TABLE II
EXPERIMENTAL RESULTS (%) ON DAYTIME-CLEAR SCENE.

Methods	Bus	Bike	Car	Motor	Person	Rider	Truck	mAP_{50}
Source-FR [7]	66.9	45.9	69.8	46.5	50.6	49.4	64.0	56.2
SW [47]	62.3	42.9	53.3	49.9	39.2	46.2	60.6	50.6
IBN-Net [34]	63.6	40.7	53.2	45.9	38.6	45.3	60.7	49.7
IterNorm [48]	58.4	34.2	42.4	44.1	31.6	40.8	55.5	43.9
ISW [35]	62.9	44.6	53.5	49.2	39.9	48.3	60.9	51.3
SDGOD [4]	68.8	50.9	53.9	56.2	41.8	52.4	68.7	56.1
CLIP-Gap [5]	55.0	47.8	67.5	46.7	49.4	46.7	54.7	52.5
UFR [6]	66.8	51.0	70.6	55.8	49.8	48.5	67.4	58.6
DINO [39]	62.6	50.7	84.3	50.8	66.5	51.7	64.5	61.6
SA-DETR	64.9	54.5	85.4	54.5	69.5	58.4	66.3	64.8

TABLE III
EXPERIMENTAL RESULTS (%) ON DUSK-RAINY SCENE.

Methods	Bus	Bike	Car	Motor	Person	Rider	Truck	mAP_{50}
FR [7]	34.2	21.8	47.9	16.0	22.9	18.5	34.9	28.0
SW [47]	35.2	16.7	50.1	10.4	20.1	13.0	38.8	26.3
IBN-Net [34]	37.0	14.8	50.3	11.4	17.3	13.3	38.4	26.1
IterNorm [48]	32.9	14.1	38.9	11.0	15.5	11.6	35.7	22.8
ISW [35]	34.7	16.0	50.0	11.1	17.8	12.6	38.8	25.9
SDGOD [4]	37.1	19.6	50.9	13.4	19.7	16.3	40.7	28.2
CLIP-Gap [5]	37.8	22.8	60.7	16.8	26.8	18.7	42.4	32.3
UFR [6]	37.1	21.8	67.9	16.4	27.4	17.9	43.9	33.2
DINO [39]	40.6	23.8	73.0	14.2	34.6	18.4	45.0	35.7
SA-DETR	50.1	31.8	77.1	28.0	50.1	27.8	52.6	45.4

Results on Daytime-Clear Scene. We first evaluate the model’s performance on the source domain. As shown in Table II, the vanilla DINO naturally surpasses CNN-based detectors, and our method further achieves a 64.8% mAP, outperforming the state-of-the-art method by 6.2%. This can be attributed to the strong ability of the DETR-based detector, as well as the effective data augmentation and the proposed OCL module, which further enhance the detector’s performance.

Results on Dusk-Rainy and Night-Rainy Scene. We evaluated our method’s performance in two unseen scenarios: “Dusk-Rainy” and “Night-Rainy”, with results presented in

TABLE IV
EXPERIMENTAL RESULTS (%) ON NIGHT-RAINY SCENE.

Methods	Bus	Bike	Car	Motor	Person	Rider	Truck	mAP_{50}
Source-FR [7]	21.3	7.7	28.8	6.1	8.9	10.3	16.0	14.2
SW [47]	22.3	7.8	27.6	0.2	10.3	10.0	17.7	13.7
IBN-Net [34]	24.6	10.0	28.4	0.9	8.3	9.8	18.1	14.3
IterNorm [48]	21.4	6.7	22.0	0.9	9.1	10.6	17.6	12.6
ISW [35]	22.5	11.4	26.9	0.4	9.9	9.8	17.5	14.1
SDGOD [4]	24.4	11.6	29.5	9.8	10.5	11.4	19.2	16.6
CLIP-Gap [5]	28.6	12.1	36.1	9.2	12.3	9.6	22.9	18.7
UFR [6]	29.9	11.8	36.1	9.4	13.1	10.5	23.3	19.2
DINO [39]	28.6	10.4	39.9	0.2	12.5	7.4	22.2	17.3
SA-DETR	34.7	14.6	47.9	0.7	23.6	12.2	27.3	23.0

TABLE V
EXPERIMENTAL RESULTS (%) ON DAYTIME-FOGGY SCENE.

Methods	Bus	Bike	Car	Motor	Person	Rider	Truck	mAP_{50}
Source-FR [7]	34.5	29.6	49.3	26.2	33.0	35.1	26.7	33.5
SW [47]	30.6	36.2	44.6	25.1	30.7	34.6	23.6	30.8
IBN-Net [34]	29.9	26.1	44.5	24.4	26.2	33.5	22.4	29.6
IterNorm [48]	29.7	21.8	42.4	24.4	26.0	33.3	21.6	28.4
ISW [35]	29.5	26.4	49.2	27.9	30.7	34.8	24.0	31.8
SDGOD [4]	32.9	28.0	48.8	29.8	32.5	38.2	24.1	33.5
CLIP-Gap [5]	36.2	34.2	57.9	34.0	38.7	43.8	25.1	38.5
UFR [6]	36.9	35.8	61.7	33.7	39.5	42.2	27.5	39.6
DINO [39]	35.1	30.1	62.8	29.0	43.3	41.3	24.4	38.0
SA-DETR	39.6	33.3	67.7	34.4	48.5	47.2	27.6	42.6

Tables III and IV. In the “Dusk-Rainy” scenario, the performance of the vanilla DINO already surpassed the best results by 2.5% mAP. Our method improved upon this, achieving a 45.4% mAP with an additional increase of 9.7%. In the Night-Rainy scenario, the vanilla DINO performs below expectations, indicating that the existing domain gap between training and testing data indeed significantly reduces the detector’s accuracy. Meanwhile, our method also demonstrated outstanding performance, achieving a 23.0% mAP, which exceeds the state-of-the-art method by a margin of 3.8% in mAP. This shows that the proposed DSA effectively enhances the detector’s robustness against significant distribution differences between the training and testing scenarios.

Results on Daytime-Foggy and Night-Clear Scene. Tables V and VI show the results of methods in two other scenarios that have smaller stylistic differences compared

TABLE VI
EXPERIMENTAL RESULTS (%) ON NIGHT-CLEAR SCENE.

Methods	Bus	Bike	Car	Motor	Person	Rider	Truck	mAP_{50}
Source-FR [7]	43.5	31.2	49.8	17.5	36.3	29.2	43.1	35.8
SW [47]	38.7	29.2	49.8	16.6	31.5	28.0	40.2	33.4
IBN-Net [34]	37.8	27.3	49.6	15.1	29.2	27.1	38.9	32.1
IterNorm [48]	38.5	23.5	38.9	15.8	26.6	25.9	38.1	29.6
ISW [35]	38.5	28.5	49.6	15.4	31.9	27.5	41.3	33.2
SDGOD [4]	40.6	35.1	50.7	19.7	34.7	32.1	43.4	36.6
CLIP-Gap [5]	37.7	34.3	58.0	19.2	37.6	28.5	42.9	36.9
UFR [6]	43.6	38.1	66.1	14.7	49.1	26.4	47.5	40.8
DINO [39]	44.1	36.9	71.0	20.2	54.8	29.9	49.0	43.7
SA-DETR	50.0	41.5	72.6	18.4	56.6	32.8	50.0	46.0

to those discussed above. The vanilla DINO also achieved competitive results, demonstrating that DETR-based detectors have better generalization for various unseen scenarios. Our method achieves the best performance, surpassing the state-of-the-art methods by 3.0% and 5.2% in mAP, respectively. These improvements are primarily achieved through the combined effects of our adapter and OCL module. The experiments demonstrate SA-DETR’s powerful capability in addressing SDG object detection tasks.

E. Visualization and Analysis

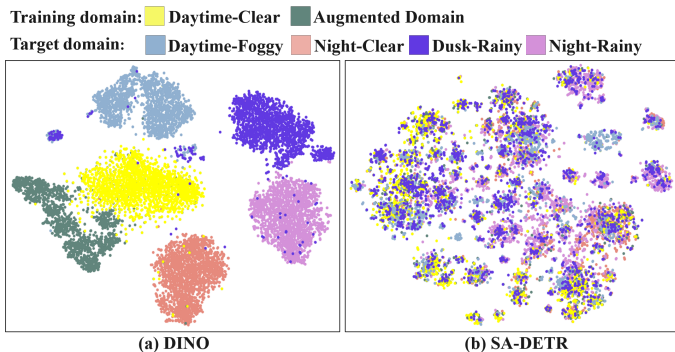


Fig. 3. The t-SNE visualization of style statistics between different domains, where the style statistics (concatenation of mean and variance) is computed from the last layer’s feature map of the ResNet-50.

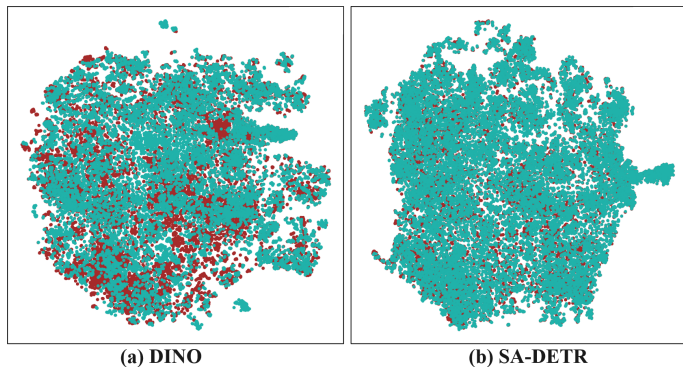


Fig. 4. The t-SNE visualization of object features from images originating from two training datasets, where red represents the source domain and green represents the augmented domain. Our OCL module aligns the domain gap well compared to the baseline method, thereby achieving predictions using instance-level domain-invariant features.

Feature visualization. We employ the t-distributed Stochastic Neighbor Embedding (t-SNE) method [49] to analyze the effectiveness of the proposed DSA and OCL module. First, we separately show the style distribution differences among various domains for the vanilla DINO and SA-DETR, as illustrated in Fig. 3. It can be observed that the style distributions across various domains are well-separated in the vanilla DINO. Conversely, our DSA projects the style representation of the target domain into the source domain, thereby entangling the style distributions across various domains. Through this dynamic adaptation to unseen scenarios, our DSA can more

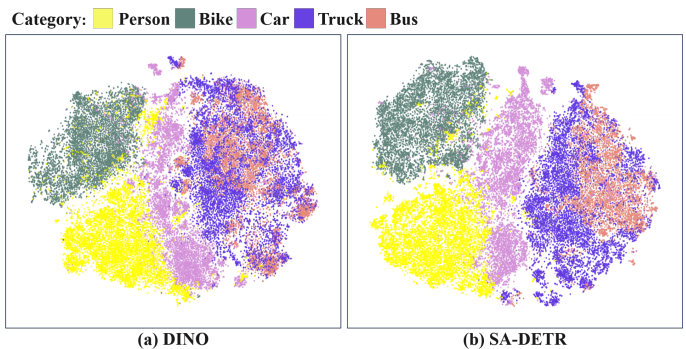


Fig. 5. The t-SNE visualization of object features from the five object categories in the Daytime-Clear images demonstrates that our detector benefits from contrastive learning, which enhances inter-category discriminability in the resultant feature space.

flexibly respond to diverse environmental changes, thereby effectively enhancing the detector’s generalization capability.

Then, we visualized the features extracted from object queries, and Fig. 4 shows that our method exhibits a minimal domain gap compared to the baseline. This demonstrates that our OCL module successfully aligns features between the source and the augmented domains, thereby achieving predictions using domain-invariant instance-level features.

Furthermore, we visualize object features by class category in the source domain, as shown in Fig. 5. This demonstrates that our detector also benefits from contrastive learning. By attracting prototypes of the same category and repelling those of different categories across domains, this approach enhances the inter-class discriminability of our detector.

Detection results. We present the visualization results of SA-DETR across all scenarios, alongside those of vanilla DINO [39], Clip-gap [5], and Groundtruth, as shown in Fig. 6. Compared to CNN-based methods, DETR-based detectors demonstrate greater accuracy in detecting small and weakly featured objects, which can be attributed to the transformer architecture’s effectiveness in capturing global structural information. Building on this, SA-DETR demonstrates more accurate classification results and higher recall rates when handling unseen scenarios, indicating that our proposed approach effectively enhances the detector’s generalization capability. The visual results align with the numerical evaluations, indicating that our method exhibits excellent performance and generalization capability in both the source domain and various unseen target domains.

V. CONCLUSION

This paper introduces the Style-Adaptive DEtection TRansformer (SA-DETR), a strong DETR-based detector designed for single-source domain generalization (SDG) in object detection. To the best of our knowledge, this is the first work that explores the benefit of a DETR-based detector for the SDG task. The SA-DETR adopts DINO as the base detector and incorporates a domain style adapter and an object-aware contrastive learning module. Firstly, the proposed adapter projects the style representation from the unseen target domain into the training domain, enabling dynamic style adaptation



Fig. 6. Our detection results compared with the state-of-the-art methods. Different categories are marked with different colors. The confidence threshold for visualization is set to 0.2. "DINO" represents the base detector that uses only source domain data for training, and "GT" stands for Ground Truth. Other descriptions represent their respective methods.

across various unseen scenarios. This establishes a new avenue that utilizes known data to represent unseen ones, thereby successfully adapting to unseen scenarios with significant differences. Then, the proposed module uses carefully designed object-aware gating masks to constrain the scope of contrastive learning in both spatial position and semantic category, forcing the detector to extract domain-invariant features of objects to further enhance the detector's generalization capability. Extensive experiments across five different weather condition scenarios show that SA-DETR achieves superior performance

for SDG in object detection. In future work, we plan to explore methods for domain adaptation during the test-time stage or under conditions of small sample sizes.

REFERENCES

- [1] Y. Chen, W. Li, C. Sakaridis, D. Dai, and L. Van Gool, "Domain adaptive faster r-cnn for object detection in the wild," in *Proceedings of the IEEE/CVF Conference on Computer Vision and Pattern Recognition*, 2018, pp. 3339–3348.
- [2] J. Zhang, J. Huang, Z. Luo, G. Zhang, X. Zhang, and S. Lu, "Dadetr: Domain adaptive detection transformer with information fusion,"

- in *Proceedings of the IEEE/CVF Conference on Computer Vision and Pattern Recognition*, 2023, pp. 23 787–23 798.
- [3] J. Yu, J. Liu, X. Wei, H. Zhou, Y. Nakata, D. Gudovskiy, T. Okuno, J. Li, K. Keutzer, and S. Zhang, “Mitrans: Cross-domain object detection with mean teacher transformer,” in *Proceedings of the European Conference on Computer Vision*, 2022, pp. 629–645.
 - [4] A. Wu and C. Deng, “Single-domain generalized object detection in urban scene via cyclic-disentangled self-distillation,” in *Proceedings of the IEEE/CVF Conference on Computer Vision and Pattern Recognition*, 2022, pp. 847–856.
 - [5] V. Vedit, M. Engilberge, and M. Salzmann, “Clip the gap: A single domain generalization approach for object detection,” in *Proceedings of the IEEE/CVF Conference on Computer Vision and Pattern Recognition*, 2023, pp. 3219–3229.
 - [6] Y. Liu, S. Zhou, X. Liu, C. Hao, B. Fan, and J. Tian, “Unbiased faster r-cnn for single-source domain generalized object detection,” in *Proceedings of the IEEE/CVF Conference on Computer Vision and Pattern Recognition*, 2024, pp. 28 838–28 847.
 - [7] S. Ren, K. He, R. Girshick, and J. Sun, “Faster r-cnn: Towards real-time object detection with region proposal networks,” *IEEE Transactions on Pattern Analysis and Machine Intelligence*, vol. 39, no. 6, pp. 1137–1149, 2017.
 - [8] W. Wang, Y. Cao, J. Zhang, F. He, Z.-J. Zha, Y. Wen, and D. Tao, “Exploring sequence feature alignment for domain adaptive detection transformers,” in *Proceedings of the ACM International Conference on Multimedia*, 2021, pp. 1730–1738.
 - [9] W.-J. Huang, Y.-L. Lu, S.-Y. Lin, Y. Xie, and Y.-Y. Lin, “Aqt: Adversarial query transformers for domain adaptive object detection,” in *Proceedings of the International Joint Conference on Artificial Intelligence*, 2022, pp. 972–979.
 - [10] Z. Zhao, S. Wei, Q. Chen, D. Li, Y. Yang, Y. Peng, and Y. Liu, “Masked retraining teacher-student framework for domain adaptive object detection,” in *Proceedings of the IEEE/CVF International Conference on Computer Vision*, 2023, pp. 19039–19049.
 - [11] N. Carion, F. Massa, G. Synnaeve, N. Usunier, A. Kirillov, and S. Zagoruyko, “End-to-end object detection with transformers,” in *Proceedings of the European Conference on Computer Vision*. Springer, 2020, pp. 213–229.
 - [12] A. Dosovitskiy, L. Beyer, A. Kolesnikov, D. Weissenborn, X. Zhai, T. Unterthiner, M. Dehghani, M. Minderer, G. Heigold, S. Gelly, J. Uszkoreit, and N. Houlsby, “An image is worth 16x16 words: Transformers for image recognition at scale,” in *Proceedings of the International Conference on Learning Representations*, 2021.
 - [13] J. Guo, N. Wang, L. Qi, and Y. Shi, “Aloft: A lightweight mlp-like architecture with dynamic low-frequency transform for domain generalization,” in *Proceedings of the IEEE/CVF Conference on Computer Vision and Pattern Recognition*, 2023, pp. 24 132–24 141.
 - [14] K. An, Y. Wang, and L. Chen, “Encouraging the mutual interact between dataset-level and image-level context for semantic segmentation of remote sensing image,” *IEEE Transactions on Geoscience and Remote Sensing*, vol. 62, no. 5606116, pp. 1–16, 2024.
 - [15] L. A. Gatys, A. S. Ecker, and M. Bethge, “Image style transfer using convolutional neural networks,” in *Proceedings of the IEEE/CVF conference on Computer Vision and Pattern Recognition*, 2016, pp. 2414–2423.
 - [16] K. Zhou, Y. Yang, Y. Qiao, and T. Xiang, “Domain generalization with mixstyle,” *arXiv preprint arXiv:2104.02008*, 2021.
 - [17] Y. Zhao, Z. Zhong, N. Zhao, N. Sebe, and G. H. Lee, “Style-hallucinated dual consistency learning for domain generalized semantic segmentation,” in *Proceedings of the European Conference on Computer Vision*. Springer, 2022, pp. 535–552.
 - [18] J. Adler and S. Lunz, “Banach wasserstein gan,” *Advances in neural information processing systems*, vol. 31, 2018.
 - [19] X. Huang and S. Belongie, “Arbitrary style transfer in real-time with adaptive instance normalization,” in *Proceedings of the IEEE/CVF International Conference on Computer Vision*, 2017, pp. 1501–1510.
 - [20] A. Vaswani, N. Shazeer, N. Parmar, J. Uszkoreit, L. Jones, A. N. Gomez, Ł. Kaiser, and I. Polosukhin, “Attention is all you need,” *Advances in neural information processing systems*, vol. 30, 2017.
 - [21] A. Neubeck and L. Van Gool, “Efficient non-maximum suppression,” in *Proceedings of the International Conference on Pattern Recognition*, 2006, pp. 850–855.
 - [22] K. Gong, S. Li, S. Li, R. Zhang, C. Liu, and Q. Chen, “Improving transferability for domain adaptive detection transformers,” in *Proceedings of the ACM International Conference on Multimedia*, 2022, pp. 1543–1551.
 - [23] Z. Tang, Y. Sun, S. Liu, and Y. Yang, “Detr with additional global aggregation for cross-domain weakly supervised object detection,” in *Proceedings of the IEEE/CVF Conference on Computer Vision and Pattern Recognition*, 2023, pp. 11 422–11 432.
 - [24] J. Han, W. Yang, Y. Wang, L. Chen, and Z. Luo, “Remote sensing teacher: Cross-domain detection transformer with learnable frequency-enhanced feature alignment in remote sensing imagery,” *IEEE Transactions on Geoscience and Remote Sensing*, vol. 62, no. 5619814, pp. 1–14, 2024.
 - [25] D. Guan, J. Huang, A. Xiao, S. Lu, and Y. Cao, “Uncertainty-aware unsupervised domain adaptation in object detection,” *IEEE Transactions on Multimedia*, vol. 24, pp. 2502–2514, 2021.
 - [26] Q. Yu, G. Irie, and K. Aizawa, “Self-labeling framework for open-set domain adaptation with few labeled samples,” *IEEE Transactions on Multimedia*, vol. 26, pp. 1474–1487, 2023.
 - [27] M. Ning, D. Lu, Y. Xie, D. Chen, D. Wei, Y. Zheng, Y. Tian, S. Yan, and L. Yuan, “Madav2: Advanced multi-anchor based active domain adaptation segmentation,” *IEEE Transactions on Pattern Analysis and Machine Intelligence*, vol. 45, no. 11, pp. 13 553–13 566, 2023.
 - [28] X. Fan, Q. Wang, J. Ke, F. Yang, B. Gong, and M. Zhou, “Adversarially adaptive normalization for single domain generalization,” in *Proceedings of the IEEE/CVF conference on Computer Vision and Pattern Recognition*, 2021, pp. 8208–8217.
 - [29] Y. Zhang, M. Li, R. Li, K. Jia, and L. Zhang, “Exact feature distribution matching for arbitrary style transfer and domain generalization,” in *Proceedings of the IEEE/CVF conference on Computer Vision and Pattern Recognition*, 2022, pp. 8035–8045.
 - [30] D. Rui, K. Guo, X. Zhu, Z. Wu, and H. Fang, “Progressive diversity generation for single domain generalization,” *IEEE Transactions on Multimedia*, pp. 1–12, 2024.
 - [31] W. Huang, C. Chen, Y. Li, J. Li, C. Li, F. Song, Y. Yan, and Z. Xiong, “Style projected clustering for domain generalized semantic segmentation,” in *Proceedings of the IEEE/CVF conference on Computer Vision and Pattern Recognition*, 2023, pp. 3061–3071.
 - [32] S. Lee, H. Seong, S. Lee, and E. Kim, “Wildnet: Learning domain generalized semantic segmentation from the wild,” in *Proceedings of the IEEE/CVF conference on Computer Vision and Pattern Recognition*, 2022, pp. 9936–9946.
 - [33] X. Li, M. Li, X. Li, and X. Guo, “Learning generalized knowledge from a single domain on urban-scene segmentation,” *IEEE Transactions on Multimedia*, vol. 25, pp. 7635–7646, 2023.
 - [34] X. Pan, P. Luo, J. Shi, and X. Tang, “Two at once: Enhancing learning and generalization capacities via ibn-net,” in *Proceedings of the European Conference on Computer Vision*, 2018, pp. 464–479.
 - [35] S. Choi, S. Jung, H. Yun, J. T. Kim, S. Kim, and J. Choo, “Robustnet: Improving domain generalization in urban-scene segmentation via instance selective whitening,” in *Proceedings of the IEEE/CVF Conference on Computer Vision and Pattern Recognition*, 2021, pp. 11 580–11 590.
 - [36] A. Radford, J. W. Kim, C. Hallacy, A. Ramesh, G. Goh, S. Agarwal, G. Sastry, A. Askell, P. Mishkin, J. Clark *et al.*, “Learning transferable visual models from natural language supervision,” in *Proceedings of the International conference on machine learning*, 2021, pp. 8748–8763.
 - [37] M. Xu, L. Qin, W. Chen, S. Pu, and L. Zhang, “Multi-view adversarial discriminator: Mine the non-causal factors for object detection in unseen domains,” in *Proceedings of the IEEE/CVF conference on Computer Vision and Pattern Recognition*, 2023, pp. 8103–8112.
 - [38] A. Kirillov, E. Mintun, N. Ravi, H. Mao, C. Rolland, L. Gustafson, T. Xiao, S. Whitehead, A. C. Berg, W.-Y. Lo *et al.*, “Segment anything,” in *Proceedings of the IEEE/CVF International Conference on Computer Vision*, 2023, pp. 4015–4026.
 - [39] H. Zhang, F. Li, S. Liu, L. Zhang, H. Su, J. Zhu, L. M. Ni, and H.-Y. Shum, “Dino: Detr with improved denoising anchor boxes for end-to-end object detection,” in *Proceedings of the International Conference on Learning Representations*, 2023.
 - [40] K. He, X. Zhang, S. Ren, and J. Sun, “Deep residual learning for image recognition,” in *Proceedings of the IEEE/CVF conference on Computer Vision and Pattern Recognition*, 2016, pp. 770–778.
 - [41] J. Su, Q. Fan, W. Pei, G. Lu, and F. Chen, “Domain-rectifying adapter for cross-domain few-shot segmentation,” in *Proceedings of the IEEE/CVF conference on Computer Vision and Pattern Recognition*, 2024, pp. 24 036–24 045.
 - [42] S. C. Marsella and J. Gratch, “Ema: A process model of appraisal dynamics,” *Cognitive Systems Research*, vol. 10, no. 1, p. 70–90, Mar 2009.
 - [43] F. Yu, H. Chen, X. Wang, W. Xian, Y. Chen, F. Liu, V. Madhavan, and T. Darrell, “Bdd100k: A diverse driving dataset for heterogeneous

- multitask learning,” in *Proceedings of the IEEE/CVF conference on Computer Vision and Pattern Recognition*, 2020, pp. 2636–2645.
- [44] M. Cordts, M. Omran, S. Ramos, T. Rehfeld, M. Enzweiler, R. Benenson, U. Franke, S. Roth, and B. Schiele, “The cityscapes dataset for semantic urban scene understanding,” in *Proceedings of the IEEE/CVF Conference on Computer Vision and Pattern Recognition*, 2016, pp. 3213–3223.
- [45] M. Hassaballah, M. A. Kenk, K. Muhammad, and S. Minaee, “Vehicle detection and tracking in adverse weather using a deep learning framework,” *IEEE Transactions on Intelligent Transportation Systems*, p. 4230–4242, 2021.
- [46] D. Kingma and J. Ba, “Adam: A method for stochastic optimization,” *arXiv preprint arXiv:1412.6980*, 2014.
- [47] X. Pan, X. Zhan, J. Shi, X. Tang, and P. Luo, “Switchable whitening for deep representation learning,” in *Proceedings of the IEEE/CVF International Conference on Computer Vision*, 2019, pp. 1863–1871.
- [48] L. Huang, Y. Zhou, F. Zhu, L. Liu, and L. Shao, “Iterative normalization: Beyond standardization towards efficient whitening,” in *Proceedings of the IEEE/CVF Conference on Computer Vision and Pattern Recognition*, 2019, pp. 4874–4883.
- [49] L. Van der Maaten and G. Hinton, “Visualizing data using t-sne.” *Journal of machine learning research*, vol. 9, no. 11, 2008.